Doping GaN NPs Synthesized by a Chemical Method for p-n Junction Application.

Motahher. A. Qaeed[1]*, A. Mindil[1], Alharthi A. Eid[1]

[1]*Department of Physical Science, Faculty of Science, University of Jeddah, Jeddah, Saudi Arabia*

[*]*Corresponding author: Motahher. A. Qaeed*

E-mail address: maqayid@uj.edu.sa Tel:+96503910717, ORCID: 0000-0002-1541-2302

Abstract: This research was devoted to studying the doping of GaN NPs at low temperature with Mg and the possibility of using them in the p-n junction. This study was subjected to a FESEM, EDX, XRD, PL and Hall Effect examination. The FESEM examination showed clear images of the NPs, the XRD peaks appear at 2θ = 32.5, 39.1 and 45.48 which conform the crystalline of p-GaN NPs, Hole Effects measurements confirm the p-GaN with different Mg ratios. The ideality factor and series resistance of p-n junction have been measured.

Keywords: P-GaN; Hall Effect; p-n junction; Magnesium; FESEM; Ideality Factor and Series Resistance

1. Introduction

Since the past two decades, III-N has been one of the most significant materials employed in applications for optoelectronic devices due to its wide, direct, adjustable bandgap capabilities in UV (0.7-6.2 eV) areas (Akasaki and Amano, 1997). GaN is a semiconductor material with a direct band gap with a width of 3.4 MeV and an excitation binding energy of 26 MeV(Amir et al., 2022). As more active areas in LEDs, high-purity gallium nitride nanoparticles make electrical devices more practical (Amir et al., 2022).

GaN NPs have been produced using a variety of techniques, including electrochemical reaction, spin coating, RF sputtering, molecular beam epitaxy, metal-organic chemical vapour deposition (MOCVD), pulsed laser deposition (PLD), and hydride vapor phase epitaxy (HVPE) (Pang and Kim, 2015, Yusoff et al., 2013, Hu et al., 2012, Joshi et al., 2010, Mantarcı and Kundakçı, 2017, Fong et al., 2015, Kawwam and Lebbou, 2014, Braniste et al., 2017, Wang et al., 2016, Qaeed et al., 2015, Qaeed et al., 2013a). The aforementioned techniques and more, some of which require vacuum as a precondition, some of which involve costly chemicals or intense heat. In our earlier research, GaN NPs were successfully produced using a chemical process that was low cost and successful at room temperature (Qaeed et al., 2013a, Qaeed et al., 2015). Due to defects like nitrogen vacancies and oxygen and hydrogen impurities that act as electrons in the electrical polarity of the alloys, high P-type doping in alloys continues to be a difficulty. Getting rid of the contaminants that lead to electro-negativity is the difficult part (Chung et al., 2010). Given its many uses, the nano-nitride composition shown a strong capacity to address this issue (Aluri et al., 2011, Qian et al., 2005) Materials like $In_xGa_{1-x}N$ with x=0.35 are typically predominantly n-type, and it is still very challenging to convert these materials to p-type by Mg doping. The findings suggest that greater background electron concentration management might lead to additional improvements in p-type conductivity in InGaN: Mg (Pantha et al., 2009). Mg-doped $In_xGa_{1-x}N$ was studied, and as the In mole percentage grew, the RT carrier concentration increased exponentially (Chen et al., 2006). By using Metal Organic Vapour phase Epitaxy with magnesium doping at 550 °C, InN and In-rich InGaN were developed. p-InGaN was produced with an acceptor concentration of 1 x 10^{19} cm^{-3}(Chang et al., 2007a). On semi-insulating c-GaN/sapphire templates, Mg-doped $In_xGa_{1-x}N$ alloys with a hole concentration ≈ 5 x10^{18} cm^{-3} and a hole mobility of 3 cm^2/V s were produced via metal organic chemical vapor deposition (Pantha et al., 2009). Due to the high activation energies (E_A) of magnesium - acceptor, a commonly accepted p-type dopant for GaN and similar alloys, where E_A rise with increase in band gap energy, it is very difficult to get highly conductive p-type GaN and AlGaN. It is advantageous to utilize P-type InGaN device structures rather than P-type GaN device structures, particularly in devices like solar cells, laser diodes, and green, long-wavelength emitters where the active area must be developed at temperatures much higher than those of the P-type GaN layer. Intense study has been put into P-

type doping of InN and In-rich InGaN. The accomplishment of their optoelectronic applications heavily rely on p-type doping. The most researched dopant functioning as a potential acceptor in InN is magnesium. Since the initial publication of evidence for p-type doping in InN and InGaN (Jones et al., 2006, Qaeed et al., 2014). In this work, we will doping GaN NPs synthesized by a chemical method via adding different amounts of magnesium to determine the best result utilize in applications

2. EXPERIMENTAL PROCEDURE

2.3 Materials: The ingredients used to create GaN NPs were obtained from Across Organics, and they are as follows: Methanol, Oleylamine (C18-content 80-90%), toluene, HNO_3 (34.5%), and NH_4OH (28-30%). Gallium (III) acetylacetonate ($Ga(acac)_3$; 99.99%) was obtained from Sigma-Aldrich.

2.4 Preparation of GaN NPs and P-Type GaN

The creation of GaN NPs involved mixing 200 mg of $Ga(acac)_3$ with 10 ml of oleylamine at room temperature. This mixture was added to a rotary evaporator flask that was placed in a 90°C water bath. After that, 10 ml of HNO_3 and 20 ml of NH_4OH were added to the solution. 12 hours were spent stirring the fluid to thoroughly dissolve the combination (Qaeed et al., 2013a). The solution was then purified five times using centrifuge equipment and 10 millilitres each of methanol and toluene. In order to create Mg-doped p-GaN NPs, 0.015 mg of MgO was dissolved in 5 ml of HNO_3. This Mg source was mixed after being added to several solutions in various amounts. To determine the samples' hole concentration, hole mobility, and resistivity, hall effect tests were carried out.

3. RESULTS AND DISCUSSIONS

In Fig. 1 (a and b), respectively, FESEM images of GaNNPs synthesized at 90°C are displayed with various scales (50 and 200 nm). According to past studies, the van der Waals forces of attraction between the particles cause the GaN NPs to aggregate (Gopalakrishnan et al., 2014, Qaeed et al., 2013b). Figure 1(c) displays the typical particle size histograms for the related FESEM picture. The geometric mean diameter of the GaN NPs, which was estimated, was found to be between 40 and 60 nm. The Scherrer equation and XR D analysis both show that the material contains aggregated nanocrystallites with near diameters. The FWHM of diffracted peaks and variations in crystallite size are factors in the Scherrer equation. However, temperature and time are important growth parameters that play a significant role in controlling the size of the GaN NPs. The results of the elemental analysis utilizing EDX measurements are displayed in Fig. 1(d), and they confirm the existence of the elements N and Ga. However, the growth factors, including temperature and time, are crucial in regulating the size of the GaN NPs. The elemental analysis performed using EDX measurement is shown in Fig. 1(d), and it verifies the presence of N and Ga elements. However, due to low temperatures, which cause the Ga to evaporate at higher temperatures, the proportion of Ga is higher than that of N(Gopalakrishnan et al., 2014).

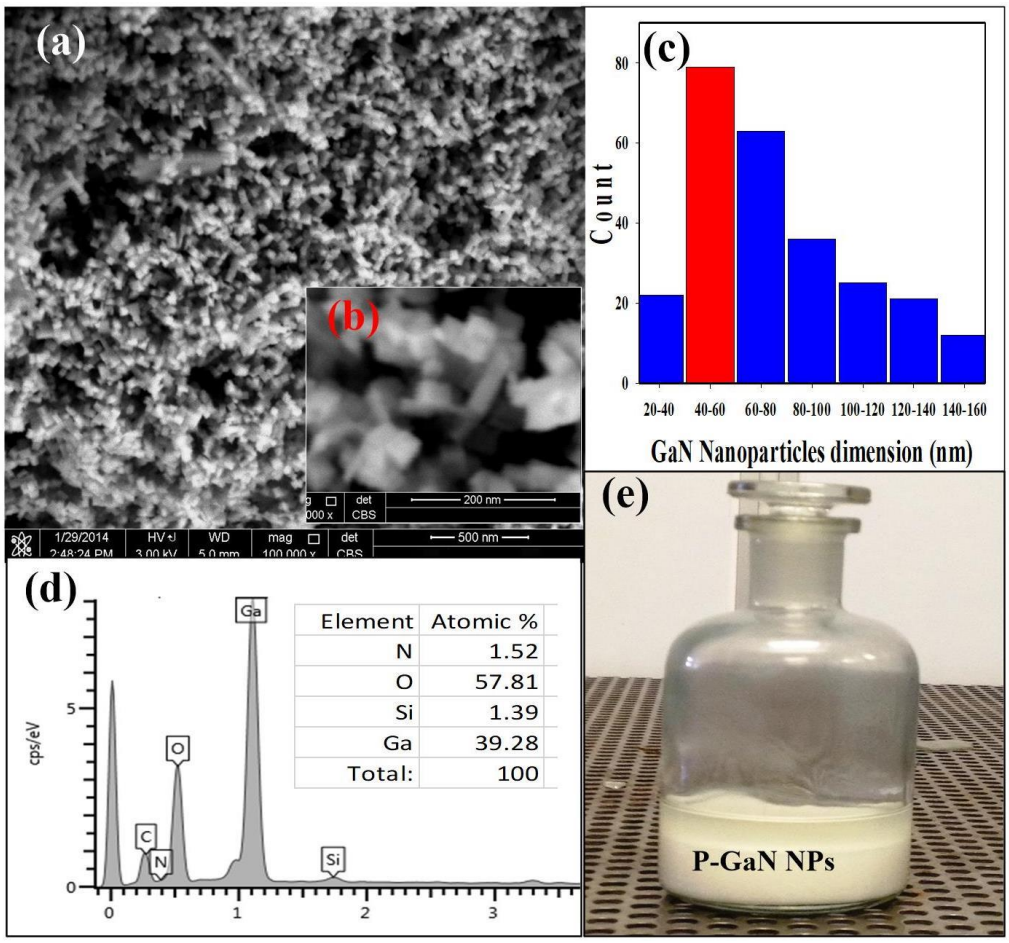

Fig.(1) p-GaN NPs synthesized by a chemical method (a) FESEM with 500nm scale (b) FESEM with 200 nm scale (c) particle size Histograms of p-GaNNPs (d) ESX of p-GaNNPs (e) image of p-GaNNPs

The samples displayed in Fig. 2 were created within eight hours using the nitrogen sources illustrated in Fig. 1: 20 ml NH_4OH and 10 ml HNO_3. The samples' high intensity peaks match the PET substrate(Qaeed et al., 2013a). The sample's findings show two c-GaN peaks at 2θ = 39.1 and 45.48 that correlate to the cubic phase and reflect from (111) and (200), as well as h-GaN nanoparticle peaks at 2θ = 32.5 that reflect from the (100) plane (Wright and Nelson, 1995, Balkaş and Davis, 1996, Falter et al., 1993). This result of the XRD result indicates that the quantity of Nitrogen source affect in the chemical reaction controls the structure formation of GaN nanoparticles. The average crystallite sizes (D_P) of the of the sample were estimated using Scherer's formula (Qaeed et al., 2013b).

$$D_P = \frac{0.9\lambda}{\rho cos\theta} \qquad (1)$$

where λ, θ and ρ are X-ray wavelength, Bragg's diffraction angle and full width at half maximum (FWHM) of the peak respectively. The average diameter of cubic and hexagonal structure of p-GaN NPs diameter was found to be approximately 55 nm.

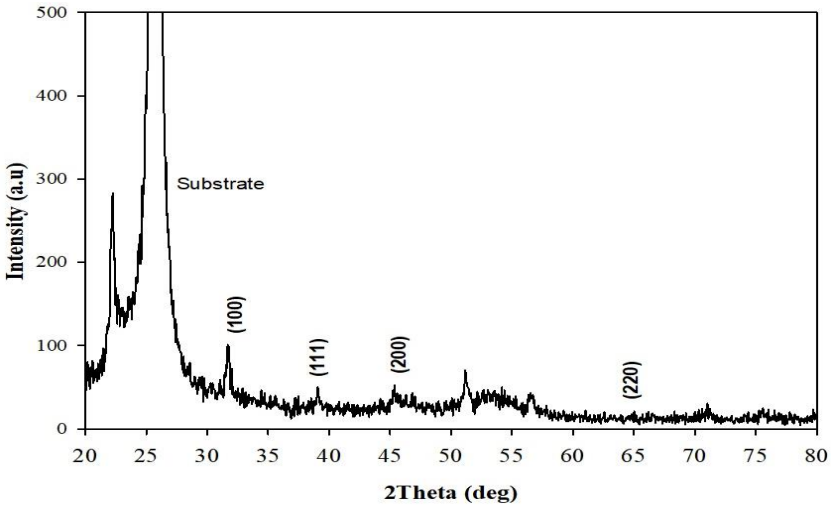

Fig.(2). XRD measurement of p-GaN NPs synthesized by a chemical method

The GaN-NPs' PL spectra are shown in the picture. GaN-NPs' PL peaks are dispersed in the UV (335–360 nm) and gradually become red when excitation wavelengths are increased. At 368 nm, the p-GaN NPs exhibit the first PL peak intensity. Doping is typically the reason for the phenomena of shifting PL peaks of NPs at various wavelengths. GaN NPs' PL peak spectra revealed another another peak between 425 and 440 nm (Hao et al., 2020). In our research, p-GaN NPs also demonstrated another peak at 435 nm with a little redshift in their spectra. The two peaks are caused by the various NP sizes. From earlier research that demonstrated that the ultraviolet PL of GaN was induced by the radiation recombination of shallow DAP (donor-accepter pairs), it may be assumed that the PL spectra are spread in the ultraviolet light range (Hao et al., 2020). Due to the very low DAP radiation recombination intensity and relatively weak PL intensity of GaN-NPs, P-GaN-NPs 368 nm UV PL is further verified.

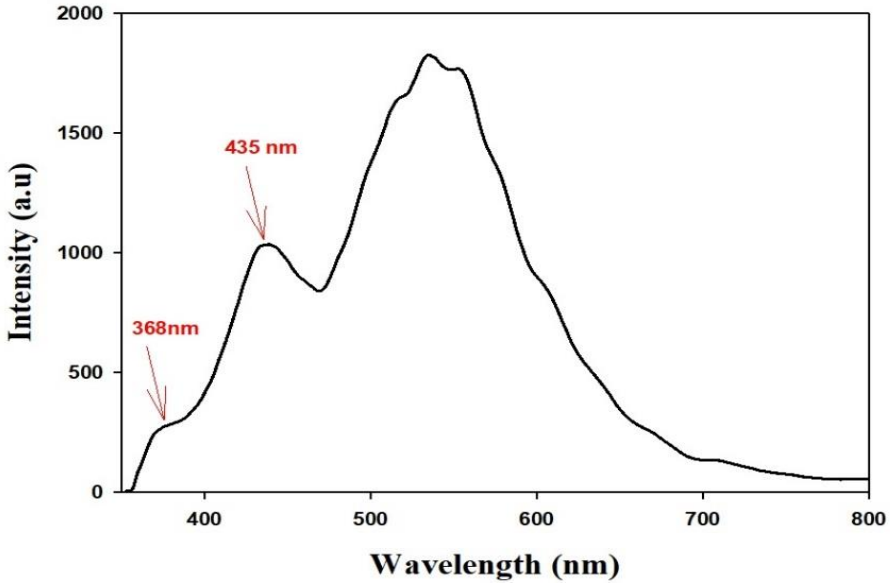

Fig.(3) Photolumenesese of p-GaN NPs synthesized by a chemical method

It takes a lot of work to get p-GaN to have a high conductivity since the Mg -acceptors that are frequently employed in doping processes have a high activation energy (E_a). Studies have demonstrated the p-type dopant's complexity in relation to p-GaN NPs. This may indicate the presence of defects like oxygen or nitrogen vacancies that are the cause of the elevated background electron concentrations (Pantha et al., 2009). The electrical characteristics of p-GaN were studied using the Hall Effect, and the hole concentration was drawn as a function of the doping ratio in Figure. The graph demonstrates how raising the dopant ratio raises resistivity and hall concentration while lowering mobility. The material's excellent quality is reflected in the sample's notable value, which results in lower values of h and higher values of h that boost the currents in optoelectronic devices, considerably enhancing device performance for a wide range of applications. The hole compensating effect by background electrons is responsible for the observed drop in hole concentration for p-GaN with a doping ratio of 0.02mg (Chang et al., 2007b).

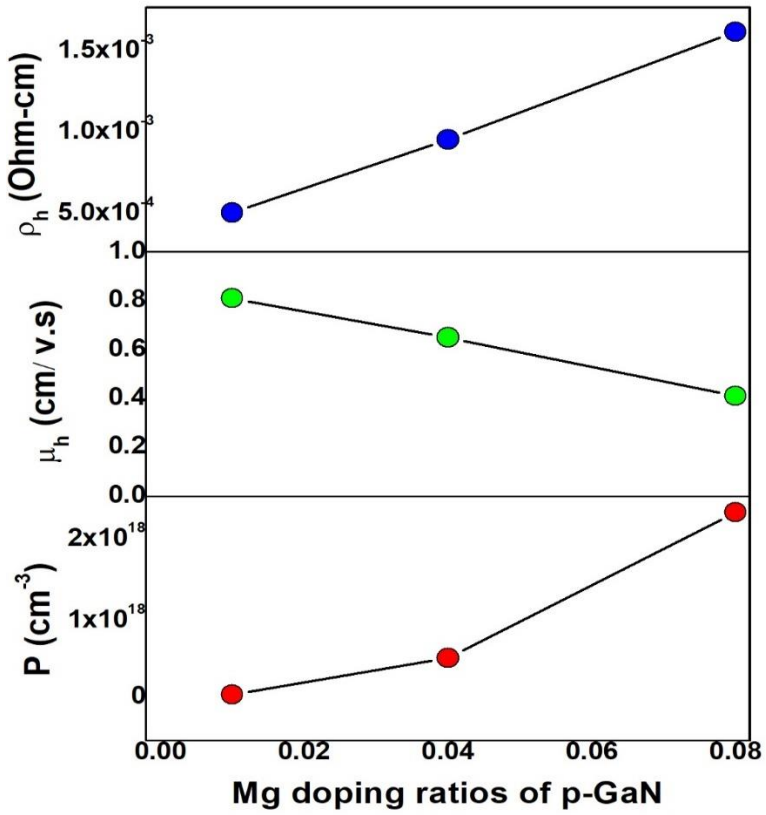

Fig. (4) Variation of the hole concentration (p), mobility (μ_h), and resistivity (ρ_h) with doping ratio of p-GaN NPs films.

The *I–V* curve of sample showed with poor rectifying behaviors because of the formation of the interfacial defects (Bhat et al., 2011, Roul et al., 2011, Miller et al., 2004). At lower voltages, it is found that the diode has a rectifying behavior. Using the standard diode Eq. (1), the diodes ideality factor *n*, barrier heights (*φB*) and saturation current density (*JS*) are extracted by fitting the forward *I-V* curves. From *I-V* curves, the values of *JS*, *φB*, and *n* are measured. The values of *n* in these hetero-junctions are found to be greater than 2, indicate that the diodes are not an ideal one. This is probably due to the presence of surface states and/or formation of an insulating layer of SiO2 at the interface (Wang, 2010). Such high values are commonly attributed to carrier tunneling via deep levels in the space charge region due to high-density localized states (Wang, 2010). The ideality factors measured in these devices however are in good agreement with that measured in GaN/Si diodes (Manna et al., 2010, Cheng et al., 2003).

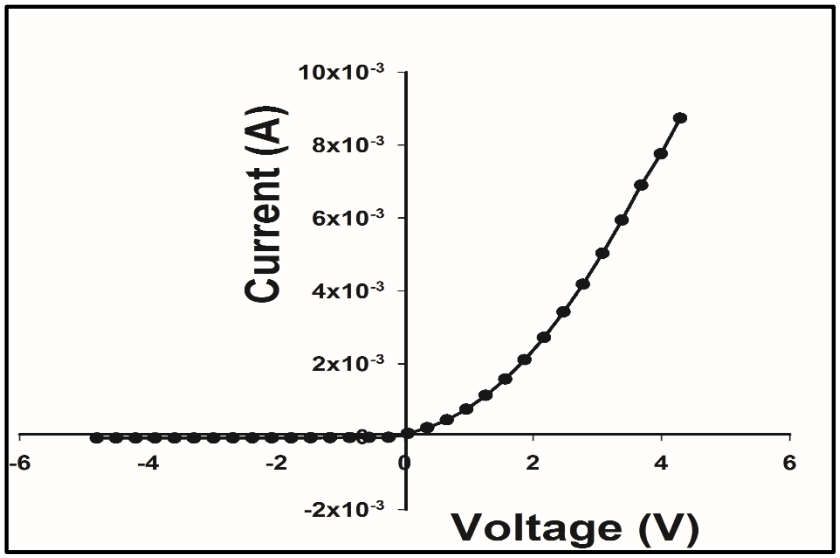

Fig. (5) Forward and reverse bias of p-n junction n-Si/p-GaN

The ideality factor of p-n junction calculated from Cheung's method where the current flows through the forward bias is given by Equation (1)

$$I = I_s e^{\frac{q(V-IR_S)}{nkT}} \quad (1)$$

$$\frac{dV}{dlog(I)} = IR_s + \frac{nkT}{q} \quad (2)$$

where R_s is the series resistance, T is the room temperature, k is the Boltzmann constant and q is the electronic charge. The ideality factor in the region suggested to be between (1-2) calculating from equation (2) and resulting from the mixture of the combined processes of diffusion and recombination processes in the neutral region and the depletion region respectively. The high value of the p-n junction ideality factor is related to the high carrier concentration (Hudait and Krupanidhi, 2001). In addition to, the high ideality factor value resulting from the high injection and series resistance effect.

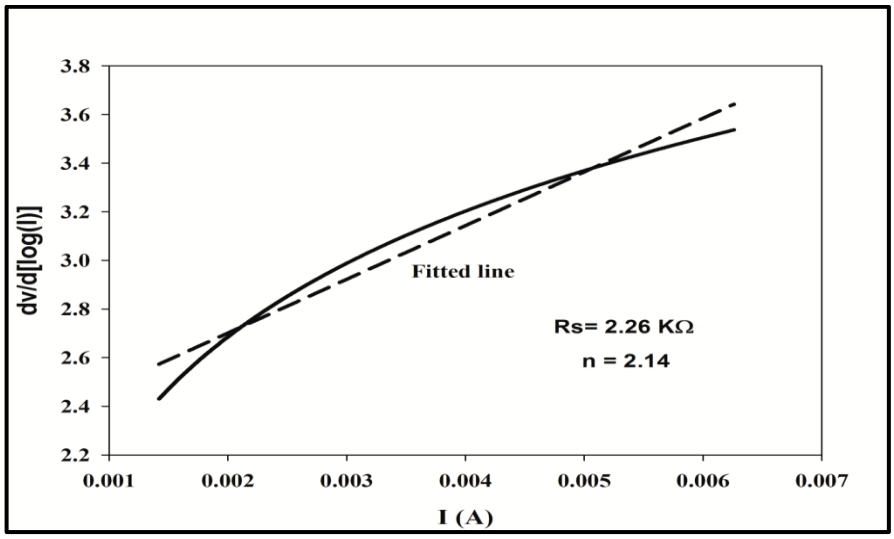

Fig. (6) Ideality factor of p-n junction calculated from Cheung's method

The barrier height (Φ_B) for p-n unction could be calculated from Eq (3)

$$\emptyset_B = \frac{kT}{q} \ln \frac{A^* T^2}{I_S} \qquad (3)$$

Wher A^* is he Richardson's constant (32 $Acm^{-2}K^{-2}$), I_s is the reverse saturation current, k is the Boltzman constant, q is the crrier charge and T is the absolute temperature. The reverse saturation currentcan be determined by extrapolating the log (I) versus Vcurve to V=0. I_s = 3.1 µA. the barrier height obtained as a little high ($\emptyset_B$= 0.689V) because it was calculated based on the higher region of forward bias voltage. In comparison with report (Gupta et al., 2009) most the carrier can flow in the forward bias of p-n junction because the lower barrier height of our p-n junction than compared report.as the forward bias showed with high current than the mentioned report.

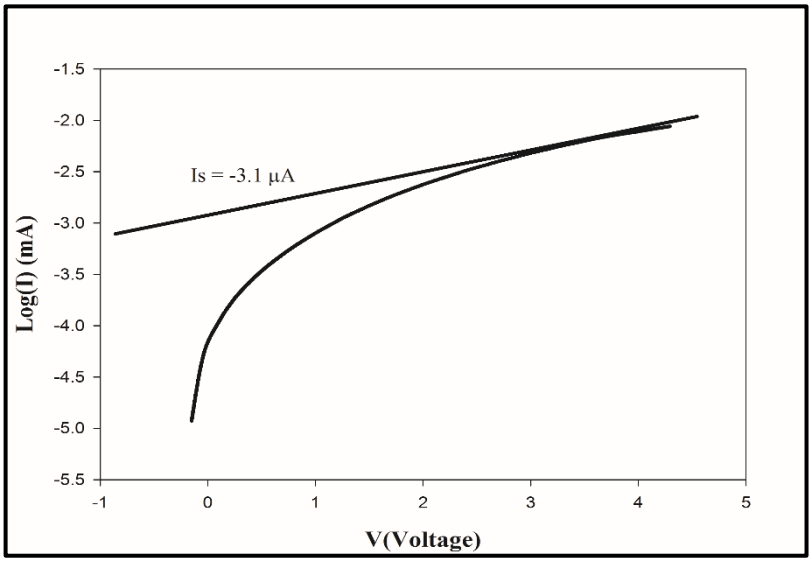

Fig. (7) Calculation the saturation current

CONCLUSION

This research presented an easy and simple method for doping gallium nitride, as well as controlling the percentage of gallium, which in turn enables us to control conductivity and resistivity, which is the greatest thing in semiconductors. The measurements demonstrated the formation of the doped p-GaN NPs and their application with n-silicon to form the p-n junction. The rectifying behaviour was proven. Finally, the study succeeded in measuring the ideality Factor and Series resistance, which made it easy to apply this method in the upcoming doping processes for the manufacture of devices such as solar cells and photodetectors.

Conflict of interest: The author declare no conflicts of interest

Acknowledgments

This work was funded by the University of Jeddah, Jeddah, Saudi Arabia, under grant No. (UJ-23-FR-64). Therefore, the authors thank the University of Jeddah for its technical and financial support.

REFERENCES

[1] Akasaki, I. A. I. & Amano, H. A. H. (1997) Crystal growth and conductivity control of group III nitride semiconductors and their application to short wavelength light emitters. *Japanese journal of applied physics,* **36** (9R)**,** 5393.

[2] Aluri, G. S., Motayed, A., Davydov, A. V., Oleshko, V. P., Bertness, K. A., Sanford, N. A. & Rao, M. V. (2011) Highly selective GaN-nanowire/TiO2-nanocluster hybrid sensors for detection of benzene and related environment pollutants. *Nanotechnology,* **22** (29)**,** 295503.

[3] Amir, H. A. A. A., Fakhri, M. A., Alwahib, A. A., Salim, E. T., Alsultany, F. H. & Hashim, U. (2022) Synthesis of gallium nitride nanostructure using pulsed laser ablation in liquid for photoelectric detector. *Materials Science in Semiconductor Processing,* **150,** 106911.

[4] Balkaş, C. M. & Davis, R. F. (1996) Synthesis routes and characterization of high-purity, single-phase gallium nitride powders. *Journal of the American Ceramic Society,* **79** (9)**,** 2309-2312.

[5] Bhat, T. N., Rajpalke, M. K., Roul, B., Kumar, M. & Krupanidhi, S. (2011) Substrate nitridation induced modulations in transport properties of wurtzite GaN/p-Si (100) heterojunctions grown by molecular beam epitaxy. *Journal of Applied Physics,* **110** (9)**,** 093718.

[6] Braniste, T., Ciers, J., Monaico, E., Martín, D., Carlin, J.-F., Ursaki, V., Sergentu, V., Tiginyanu, I. & Grandjean, N. (2017) Multilayer porous structures of HVPE and MOCVD grown GaN for photonic applications. *Superlattices and Microstructures,* **102,** 221-234.

[7] Chang, C.-A., Tang, T.-Y., Chang, P.-H., Chen, N.-C. & Liang, C.-T. (2007a) Magnesium doping of In-rich InGaN. *Japanese journal of applied physics,* **46,** 2840.

[8] Chang, C.-A., Tang, T.-Y., Chang, P.-H., Chen, N.-C. & Liang, C.-T. (2007b) Magnesium doping of In-rich InGaN. *Japanese journal of applied physics,* **46** (5R)**,** 2840.

[9] Chen, P.-C., Chen, C.-H., Chang, S.-J., Su, Y.-K., Chang, P.-C. & Huang, B.-R. (2006) High hole concentration of p-type InGaN epitaxial layers grown by MOCVD. *Thin Solid Films,* **498** (1)**,** 113-117.

[10] Cheng, G., Kolmakov, A., Zhang, Y., Moskovits, M., Munden, R., Reed, M. A., Wang, G., Moses, D. & Zhang, J. (2003) Current rectification in a single GaN nanowire with a well-defined p–n junction. *Applied Physics Letters,* **83** (8)**,** 1578-1580.

[11] Chung, K., Lee, C.-H. & Yi, G.-C. (2010) Transferable GaN layers grown on ZnO-coated graphene layers for optoelectronic devices. *science,* **330** (6004)**,** 655-657.

[12] Falter, C., Klenner, M. & Chen, Q. (1993) Role of bonding, reduced screening, and structure in the high-temperature superconductors. *Physical Review B,* **48** (22)**,** 16690.

[13] Fong, C., Ng, S., Yam, F., Hassan, H. A. & Hassan, Z. (2015) Growth of GaN on sputtered GaN buffer layer via low cost and simplified sol–gel spin coating method. *Vacuum,* **119,** 119-122.

[14] Gopalakrishnan, M., Purushothaman, V., Ramakrishnan, V., Bhalerao, G. & Jeganathan, K. (2014) The effect of nitridation temperature on the structural, optical and electrical properties of GaN nanoparticles. *CrystEngComm,* **16** (17)**,** 3584-3591.

[15] Gupta, R., Ghosh, K. & Kahol, P. (2009) Fabrication and characterization of NiO/ZnO p–n junctions by pulsed laser deposition. *Physica E: Low-dimensional Systems and Nanostructures,* **41** (4)**,** 617-620.

[16] Hao, J., Xu, S., Gao, B. & Pan, L. (2020) PL tunable GaN nanoparticles synthesis through femtosecond pulsed laser ablation in different environments. *Nanomaterials,* **10** (3)**,** 439.

[17] Hu, Q., Wei, T., Duan, R., Yang, J., Huo, Z., Zeng, Y. & Xu, S. (2012) Polarity dependent structure and optical properties of freestanding GaN layers grown by hydride vapor phase epitaxy. *Materials Science in Semiconductor Processing,* **15** (1)**,** 15-19.

[18] Hudait, M. & Krupanidhi, S. (2001) Doping dependence of the barrier height and ideality factor of Au/n-GaAs Schottky diodes at low temperatures. *Physica B: Condensed Matter,* **307** (1)**,** 125-137.

[19] Jones, R., Yu, K., Li, S., Walukiewicz, W., Ager, J., Haller, E., Lu, H. & Schaff, W. (2006) Evidence for p-type doping of InN. *Physical review letters,* **96** (12)**,** 125505.

[20] Joshi, B. C., Mathew, M., Joshi, B., Kumar, D. & Dhanavantri, C. (2010) Characterization of GaN/AlGaN epitaxial layers grown by metalorganic chemical vapour deposition for high electron mobility transistor applications. *Pramana,* **74** (1)**,** 135-141.

[21] Kawwam, M. & Lebbou, K. (2014) The influence of deposition parameters on the structural quality of PLD-grown GaN/sapphire thin films. *Applied Surface Science,* **292,** 906-914.

[22] Manna, S., Ashok, V. D. & De, S. (2010) Rectifying properties of p-GaN nanowires and an n-silicon heterojunction vertical diode. *ACS applied materials & interfaces,* **2** (12)**,** 3539-3543.

[23] Mantarcı, A. & Kundakçı, M. (2017) Some of structural and morphological optimization of GaN thin film on Si (100) substrate grown by RF sputter. *AIP Conference Proceedings.* AIP Publishing LLC.

[24] Miller, E., Yu, E., Waltereit, P. & Speck, J. (2004) Analysis of reverse-bias leakage current mechanisms in GaN grown by molecular-beam epitaxy. *Applied Physics Letters,* **84** (4)**,** 535-537.

[25] Pang, L. & Kim, K. K. (2015) Improvement of Ohmic contacts to n-type GaN using a Ti/Al multi-layered contact scheme. *Materials Science in Semiconductor Processing,* **29,** 90-94.

[26] Pantha, B., Sedhain, A., Li, J., Lin, J. & Jiang, H. (2009) Electrical and optical properties of p-type InGaN. *Applied physics letters,* **95** (26)**,** 261904.

[27] Qaeed, M., Ibrahim, K., Saron, K., Ahmed, M. & Allam, N. K. (2014) Low-temperature solution-processed flexible solar cells based on (In, Ga) N nanocubes. *ACS applied materials & interfaces,* **6** (13)**,** 9925-9931.

[28] Qaeed, M., Ibrahim, K., Saron, K., Mukhlif, M., Ismail, A., Elfadill, N. G., Chahrour, K. M., Abdullah, Q. & Aldroobi, K. (2015) New issue of GaN nanoparticles solar cell. *Current Applied Physics,* **15** (4)**,** 499-503.

[29] Qaeed, M., Ibrahim, K., Saron, K. & Salhin, A. (2013a) Cubic and hexagonal GaN nanoparticles synthesized at low temperature. *Superlattices and Microstructures,* **64,** 70-77.

[30] Qaeed, M., Ibrahim, K., Srivastava, R., Ali, M. & Salhin, A. (2013b) Structural and optical characterization of InGaN nanoparticles synthesized at low temperature. *Materials Letters,* **99,** 128-130.

[31] Qian, F., Gradecak, S., Li, Y., Wen, C.-Y. & Lieber, C. M. (2005) Core/multishell nanowire heterostructures as multicolor, high-efficiency light-emitting diodes. *Nano letters,* **5** (11)**,** 2287-2291.

[32] Roul, B., Kumar, M., Rajpalke, M. K., Bhat, T. N., Sinha, N., Kalghatgi, A. & Krupanidhi, S. (2011) Effect of N/Ga flux ratio on transport behavior of Pt/GaN Schottky diodes. *Journal of Applied Physics,* **110** (6)**,** 064502.

[33] Wang, M., Bian, J., Sun, H., Liu, W., Zhang, Y. & Luo, Y. (2016) n-VO2/p-GaN based nitride–oxide heterostructure with various thickness of VO2 layer grown by MBE. *Applied Surface Science,* **389,** 199-204.

[34] Wang, Z. L. (2010) Piezopotential gated nanowire devices: Piezotronics and piezo-phototronics. *Nano Today,* **5** (6)**,** 540-552.

[35] Wright, A. & Nelson, J. (1995) Consistent structural properties for AlN, GaN, and InN. *Physical Review B,* **51** (12)**,** 7866.

[36] Yusoff, M. M., Hassan, Z., Ahmed, N. M., Hassan, H. A., Abdullah, M. & Rashid, M. (2013) pn-Junction photodiode based on GaN grown on Si (111) by plasma-assisted molecular beam epitaxy. *Materials Science in Semiconductor Processing,* **16** (6)**,** 1859-1864.

DOI: https://doi.org/10.15379/ijmst.v10i3.3367